A thermodynamic description for physiological transmembrane transport

Marco Arieli Herrera-Valdez [1]✉
[1] Facultad de Ciencias, Universidad Nacional Autónoma de México

✉$marcoh@ciencias.unam.mx$

April 16, 2018

Abstract

Physiological mechanisms for passive and active transmembrane transport have been theoretically described using many different approaches. A generic formulation for both passive and active transmembrane transport, is derived from basic thermodynamical principles taking into account macroscopic forward and backward molecular fluxes, relative to a source compartment, respectively. Electrogenic fluxes also depend on the transmembrane potential and can be readily converted into currents. Interestingly, the conductance-based formulation for current is the linear approximation of the generic formulation for current, around the reversal potential. Also, other known formulas for current based on electrodiffusion turn out to be particular examples of the generic formulation. The applicability of the generic formulations is illustrated with models of transmembrane potential dynamics for cardiocytes and neurons. The generic formulations presented here provide a common ground for the biophysical study of physiological phenomena that depend on transmembrane transport.

1 Introduction

One of the most important physiological mechanisms underlying communication within and between cells is the transport of molecules across membranes. Molecules can cross membranes either passively (Stein and Litman, 2014), or via active transport (Bennett, 1956). Passive transmembrane transport occurs through pores that may be spontaneously formed within the lipid bilayer (Blicher and Heimburg, 2013), or within transmembrane proteins called channels (Hille, 1992; Stein and Litman, 2014) that may be selective for particular ion types (Almers and McCleskey, 1984; Doyle et al., 1998; Favre et al., 1996). In contrast, active transport is mediated by transmembrane proteins that mechanically translocate at least one ion type against its electrochemical gradient (Bennett, 1956; Ussing, 1949a,c). These proteins are also called pumps and use energy from biochemical reactions (e.g. ATPases, light-driven pumps) or from the electrochemical gradients of other ions (e.g. symporters, exchangers) (SKou, 1965). One important functional distinction between channels and pumps is that the rate of transport for channels is several orders of magnitude faster than the rate for pump-mediated transport (Gadsby, 2009; Herrera-Valdez and Lega, 2011; Ussing, 1949b) .

Theoretical models of transmembrane transport play a critical role in developing our understanding of the function and the mechanisms underlying electrical signaling and cellular excitability (Barr, 1965; Cole, 1965; DiFrancesco and Noble, 1985; Endresen et al., 2000; Gadsby, 2009; Goldman, 1943; Kell, 1979; Läuger, 1973; Stevens and Tsien, 1979; Wiggins, 1985a,b,c). The best known transmembrane transport

PeerJ Preprints | https://doi.org/10.7287/peerj.preprints.1312v8 | CC BY 4.0 Open Access | rec: 16 Apr 2018, publ: 16 Apr 2018

models include the widely used conductance-based formulation from the seminal work of Hodgkin and Huxley (1952), the Goldman-Hodgkin-Katz equation (Goldman, 1943; **?**; **?**), and several other expressions for carrier and channel mediated transport with many different functional forms (DiFrancesco and Noble, 1985; Herrera-Valdez and Lega, 2011; Rasmusson et al., 1990a,b; Rosenberg and Wilbrandt, 1955). To the author's knowledge, the most general formulations for *ionic* transport across membranes available in the literature include those in the seminal work by **??**, **?** (see also (**?**)), similar work by (Endresen et al., 2000), and those in the excellent book by Johnston et al. (1995). Such formulations describe the relationship between the activity and permeability of ions across membranes, and the transmembrane potential. However generalizations to describe physiological transport at large, including non-charged molecules, are still missing. The work presented here builds upon the results previously mentioned, describing transmembrane transport macroscopically in terms of the energy required to move molecules across a membrane. The result is a generic formulation with a functional form that is common for both passive and active transport of molecules across membranes (Herrera-Valdez, 2014). Fits from experimental data can be readily obtained using these formulations to construct a model of transmembrane potential dynamics (Herrera-Valdez et al., 2013).

The details of the derivation can be found in the next section. A model of membrane potential dynamics in cardiac pacemaker cells can be found in Section 3. A model of fast spiking interneuron dynamics based on the same equations is also included in the Appendix A.

2 Generic formulation for transmembrane flux and current

2.1 Work required for transmembrane ionic fluxes

Consider a system with two aqueous compartments separated by a membrane and regard one of the compartments as a source and the other as a target. Assume that the two compartments contain ions of the same type and that the membrane is permeable to those ions. Let α and β represent source→target (forward) and source←target (backward) fluxes. Explicitly,

$$\alpha = r_\alpha \exp\left(-\frac{E_\alpha}{\mathrm{kT}}\right), \tag{1}$$

$$\beta = r_\beta \exp\left(-\frac{E_\beta}{\mathrm{kT}}\right), \tag{2}$$

as described by the van Hoff-Arrhenius equation (Arrhenius, 1889; van't Hoff, 1884), where r_α and r_β are flow rates (molecules ms$^{-1}\mu\, m^{-2}$); E_α and E_β are the energies required for the molecules to cross in the forward and backward direction; k is Boltzmann's constant and T is the absolute temperature, respectively. Let $\Delta G = E_\alpha - E_\beta$ represent the work required for the transport. The energies E_α and E_β can be assumed to depend on the concentrations of the molecules, and if the molecules are ions, on the electrical potential across the membrane. If the energy is continuous as a function of space, there is a $b \in [0,1]$ such that

$$E_\alpha = b\Delta G, \quad \text{and} \quad E_\beta = -(1-b)\Delta G. \tag{3}$$

The rates α and β can then be rewritten in terms of ΔG,

$$\alpha = r_\alpha \exp\left(-b\frac{\Delta G}{\mathrm{kT}}\right), \qquad \beta = r_\beta \exp\left((1-b)\frac{\Delta G}{\mathrm{kT}}\right). \tag{4}$$

The parameter $b \in [0,1]$ can be thought of as a bias for the transport in the forward direction when close to 1, and in the backward direction when close to 0 (Butler, 1924; Erdey-Grúz and Volmer, 1930; Herrera-Valdez, 2014; Wiggins, 1985a). The ratio between the forward and backward fluxes at steady

PeerJ Preprints | https://doi.org/10.7287/peerj.preprints.1312v8 | CC BY 4.0 Open Access | rec: 16 Apr 2018, publ: 16 Apr 2018

state should then be such that

$$\frac{\alpha}{\beta} = \exp\left(-\frac{\Delta G}{\mathrm{kT}}\right), \tag{5}$$

which means that $r_\alpha = r_\beta$, and the *flux* associated to the transmembrane transport taking the source compartment as a reference can then be written as

$$\alpha - \beta = r\left[\exp\left(-b\frac{\Delta G}{\mathrm{kT}}\right) - \exp\left((1-b)\frac{\Delta G}{\mathrm{kT}}\right)\right], \tag{6}$$

with r in units of molecules millisecond^{-1} μm^{-2}. The rate r should larger for electrodiffusive transport in comparison to the slower transport rates for pumps and other carrier proteins. There is experimental evidence for some ion channels that supports the replacement of r as a constant (Nonner and Eisenberg, 1998). It is possible, however, to derive expressions for r that take into account biophysical variables like temperature and the shape and length of the pore through which the ions cross (Endresen et al., 2000; **?**).

The applicability of the generic formulation for transmembrane flux (equation (6)) depends on whether it is possible to calculate ΔG for different transport mechanisms. The following section shows how to calculate, explicit expressions for ΔG in terms of the concentrations of the transported molecules and the transmembrane potential if they are charged. These calculations can then be extended to calculate the energy required for different passive and active transmembrane transport mechanisms involving different types of molecules in parallel.

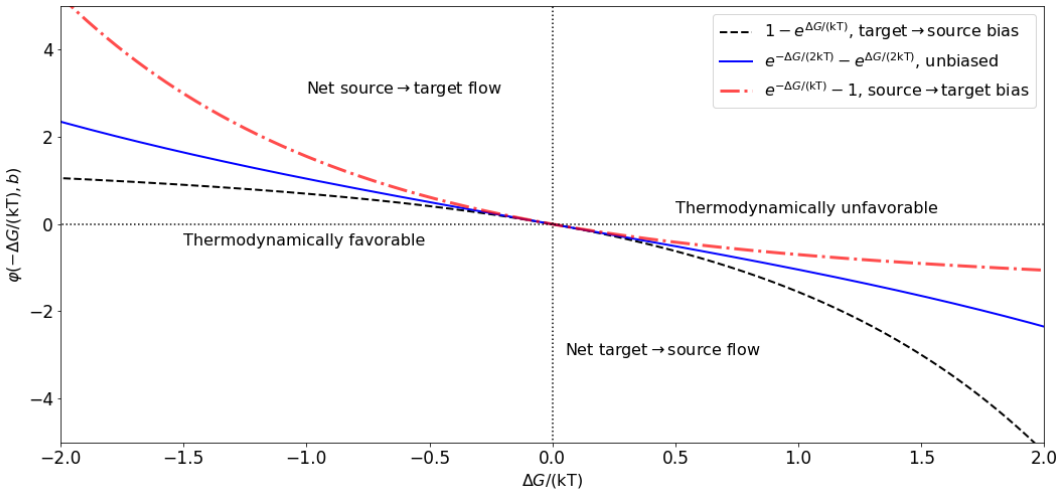

Figure 1: Fluxes biased in the target→source (b=0.1, black dashed line), source→target (b=0.9, red dash-dot line), or showing no rectification (b=0.5, blue solid line). See Table 1 for examples.

2.2 Transmembrane transport of molecules of the same type

Assume that molecules of type s (*e.g.* K^+) are able to cross the membrane and that ΔG_s is the energy for required for their transport across the membrane. To take the direction of motion into account, label the extracellular and intracellular compartments as 0 and 1, respectively, and let c_s and d_s represent the source and the destination compartments for the transport of the s-molecules. The pair (c_s, d_s)=(0,1)

PeerJ Preprints | https://doi.org/10.7287/peerj.preprints.1312v8 | CC BY 4.0 Open Access | rec: 16 Apr 2018, publ: 16 Apr 2018

represents inward transport and the pair (c_s, d_s)=(1,0) represents outward transport. The work required to transport n_s molecules of type s from compartment c_s to compartment d_s can then be expressed as

$$\Delta G_s = n_s \left(c_s - d_s\right) \left[\mathrm{kT} \ln\left(\frac{[s]_0}{[s]_1}\right) - \mathrm{q} z_s v\right], \tag{7}$$

(Aidley, 1998; Blaustein et al., 2004; Weer et al., 1988) where q, z_s, $[s]_0$, and $[s]_1$ represent the elementary charge, the valence, the extracellular, and the intracellular concentrations for the molecules of type s, respectively. If the s-molecules are not charged, $z_s = 0$ and the work required to move the s-type molecules from c_s to d_s simplifies to

$$\Delta G_s = n_s \left(c_s - d_s\right) \mathrm{kT} \ln\left(\frac{[s]_0}{[s]_1}\right).$$

For ions, $z_s \neq 0$, and equation (7) can be rewritten as

$$\Delta G_s = \mathrm{q} z_s n_s \left(c_s - d_s\right) \left(v_s - v\right), \tag{8}$$

where v_s is the transmembrane potential at which there is a zero net flux of s-ions across the membrane (Nernst, 1888). If $\Delta G_s < 0$, $s \in 1, ..., m$, then the molecules can be transported passively (*e.g.* electrodiffusion), thus freeing energy stored in their electrochemical gradient. In contrast, if $\Delta G_s > 0$, the transmembrane transport of the s-molecules from c_s to d_s is not thermodynamically favorable, which means the transport from c_s to d_s must be active (*e.g.* pumping), and it increases the electrochemical gradient of s if it happens.

2.3 Joint transmembrane transport of molecules of different types

To find a generic expression for ΔG in equation (6), consider a generic transport mechanism by which m different types of molecules move across the membrane (*e.g.* for Na^+-Ca^{2+} exchange, $m = 2$) according to equation (7). Let $M = \{1, ..., m\}$ represent a set for the types of molecules undergoing transport in parallel. The total energy required for the transport the molecules is the sum of the energies required to transport each type of molecule. In other words,

$$\Delta G_M = \sum \left\{\Delta G_s : s \in M\right\}. \tag{9}$$

Not all the molecules may not be transported in the same direction and also, molecules may be transported against their (electro)chemical gradient. Those molecules that are transported in a thermodynamically unfavorable direction form a set $U = \{s \in M : \Delta G_s > 0\}$. The (simultaneous) transmembrane transport of the molecules in M is called *passive* if $U = \emptyset$, and active if not. *Primary active* transport is such that at least one of the molecular types in M is transported against its electrochemical gradient, and also, such that the energy required to pump the molecules from the set U is larger than the energy stored in the electrochemical gradients of those molecules from not in U. That is,

$$\sum \left\{\Delta G_s : s \in U\right\} > \sum \left\{\Delta G_s : s \in M \setminus U\right\}. \tag{10}$$

In physiological systems, the extra energy required for the transport is supplied by different mechanisms like ATP hydrolysis (Fleischer and Fleischer, 1988) and light transduction (Lanyi, 1993). In contrast, *secondary active* transport is such that the energy stored in the electrochemical gradients of those molecules not in U is larger than the energy required to pump the molecules from U. Explicitly,

$$\sum \left\{\Delta G_s : s \in U\right\} < \sum \left\{\Delta G_s : s \in M \setminus U\right\}, \tag{11}$$

If the transport is passive or secondary active, $\Delta G_M < 0$, and the energy required for the transport is supplied by the electrochemical gradients of the molecules that are not in U. In contrast, $\Delta G_M > 0$ for

PeerJ Preprints | https://doi.org/10.7287/peerj.preprints.1312v8 | CC BY 4.0 Open Access | rec: 16 Apr 2018, publ: 16 Apr 2018

primary active transport. This means that the transport can only be done by adding an external source of energy ΔG_{Ext}, which must be large enough so that $\Delta G_M + \Delta G_{\mathrm{Ext}}$ becomes negative. Taking the above remarks into account, write the total energy for the transport as

$$\Delta G = \delta_{\mathrm{Ext}} \Delta G_{\mathrm{Ext}} + \Delta G_M, \tag{12}$$

where $\delta_{\mathrm{Ext}} = 1$ when $\Delta G_M > 0$, and 0 otherwise. In particular, for ATP-driven transport, the free energy from the breakdown of ATP can be written as (Tanford, 1981; Weer et al., 1988)

$$\Delta G_{\mathrm{ATP}} = \mathrm{q}\left[\Delta G^0_{\mathrm{ATP}} + \frac{\mathrm{kT}}{\mathrm{q}} \ln\left(\frac{[\mathrm{ADP}]\,[\mathrm{P}_i]}{[\mathrm{ATP}]}\right)\right] = \mathrm{q} v_{\mathrm{ATP}}, \tag{13}$$

where $v_{\mathrm{ATP}} \approx -450$ mV (Endresen et al., 2000; Weer et al., 1988), but could vary depending on the amounts of ATP, ADP, and P_i. Similar expressions could be derived active transport driven by light, or other sources of energy, so that $\Delta G_{\mathrm{Ext}} = \mathrm{q} v_{\mathrm{Ext}}$.

Taking the above observations into account, it is possible to combine equations (9) and (12), and write α/β from equation (5) as

$$\exp\left(-\frac{\Delta G}{\mathrm{kT}}\right) = \exp\left(\frac{\eta v - \delta_{\mathrm{Ext}} v_{\mathrm{Ext}}}{v_{\mathrm{T}}}\right) \prod_{s=1}^{m} \left(\frac{[s]_0}{[s]_1}\right)^{n_s(d_s - c_s)} \tag{14}$$

where $v_{\mathrm{T}} = \mathrm{kT}/\mathrm{q}$, and

$$\eta = \sum_{s=1}^{m} n_s \left(c_s - d_s\right) z_s. \tag{15}$$

represents the net number of charges moved across the membrane. The product $\mathrm{q}\eta$ (in Coulombs) represents the net charge moved across the membrane, relative to the extracellular compartment. As a consequence, if $\eta = 0$, then transport is non-electrogenic and does not depend on the transmembrane potential.

Transmembrane transport of ions. If the transport only involves ions, then equation (14) can be simplified to

$$\exp\left(-\frac{\Delta G}{\mathrm{kT}}\right) = \exp\left(\frac{\eta v - v_o}{v_{\mathrm{T}}}\right) \tag{16}$$

with

$$v_o = \delta_{\mathrm{Ext}} v_{\mathrm{Ext}} + \sum_{s=1}^{m} n_s z_s \left(c_s - d_s\right) v_s. \tag{17}$$

The quantity v_o/η can be thought of as a reversal potential. If $\eta > 0$, then positive charge is transported inward, or negative charge is transported outward. In contrast, $\eta > 0$ means that positive charge is transported outward or negative charge transported inward. For instance, inward electrodiffusion of single Na^+ ions gives an $\eta = -1$, which can be thought of as loosing one positive charge at a time from the extracellular compartment (see Table 1). More in general, if transport is electrodiffusive and carried by a single ion of type l (as it would be in channels permeable to ions of type l), v_o reduces to $\eta_l v_l$ where v_l is the Nernst potential for ions of type l. A list with examples of energies and total charge movements for different transport mechanisms can be found Table 1.

2.4 Flux and current

The normalized energy for the possibly simultaneous transmembrane transport of ions of m different types (equation (16)) can be used to describe their transmembrane flux and also the current when the transport is electrogenic.

PeerJ Preprints | https://doi.org/10.7287/peerj.preprints.1312v8 | CC BY 4.0 Open Access | rec: 16 Apr 2018, publ: 16 Apr 2018

Table 1: Energy required for transmembrane ionic transport mediated by different passive and active mechanisms.

Pump or channel	Ion (s)	n_s	c_s	d_s	$c_s - d_s$	$\Delta G_s = \mathrm{q} n_s (c_s - d_s)\left[v_\mathrm{T} \log\left(\frac{[s]_0}{[s]_1}\right) - z_s v\right]$	η	v_o	$\alpha/\beta = \exp\left(-\frac{\Delta G}{\mathrm{kT}}\right)$
Cl^- channel	Cl^-	1	0	1	-1	$\Delta G_\mathrm{Cl} = \mathrm{q}(v_\mathrm{Cl} - v)$	1	v_Cl	$\left(\frac{[Cl]_1}{[Cl]_0}\right) \exp\left(\frac{v}{v_\mathrm{T}}\right)$
K^+ channel	K^+	1	1	0	1	$\Delta G_\mathrm{K} = \mathrm{q}(v_\mathrm{K} - v)$	1	v_K	$\left(\frac{[\mathrm{K}]_1}{[\mathrm{K}]_0}\right) \exp\left(\frac{v}{v_\mathrm{T}}\right)$
Na^+ channel	Na^+	1	0	1	-1	$\Delta G_\mathrm{Na} = -\mathrm{q}(v_\mathrm{Na} - v)$	-1	$-v_\mathrm{Na}$	$\left(\frac{[Na]_0}{[Na]_1}\right) \exp\left(-\frac{v}{v_\mathrm{T}}\right)$
Ca^{2+} channel	Ca^{2+}	1	0	1	-1	$\Delta G_\mathrm{Ca} = -2\mathrm{q}(v_\mathrm{Ca} - v)$	-2	$-2v_\mathrm{Ca}$	$\left(\frac{[Ca]_0}{[Ca]_1}\right) \exp\left(-2\frac{v}{v_\mathrm{T}}\right)$
Na^+-K^+ ATPase	Na^+ K^+	3 2	1 0	0 1	1 -1	$\Delta G_\mathrm{Na} = 3\mathrm{q}(v_\mathrm{Na} - v)$ $\Delta G_\mathrm{K} = -2\mathrm{q}(v_\mathrm{K} - v)$	1	$v_\mathrm{ATP} + 3v_\mathrm{Na} - 2v_\mathrm{K}$	$\left(\frac{[\mathrm{Na}]_1}{[\mathrm{Na}]_0}\right)^3 \left(\frac{[\mathrm{K}]_0}{[\mathrm{K}]_1}\right)^2 \exp\left(\frac{v - v_\mathrm{ATP}}{v_\mathrm{T}}\right)$
Ca^{2+} ATPase	Ca^{2+}	1	1	0	1	$\Delta G_\mathrm{Ca} = 2\mathrm{q}(v_\mathrm{Ca} - v)$	2	$v_\mathrm{ATP} + 2v_\mathrm{Ca}$	$\left(\frac{[Ca]_1}{[Ca]_0}\right) \exp\left(\frac{2v - v_\mathrm{ATP}}{v_\mathrm{T}}\right)$
H^+ ATPase	H^+	1	1	0	1	$\Delta G_\mathrm{H} = \mathrm{q}(v_\mathrm{H} - v)$	1	$v_\mathrm{ATP} + v_\mathrm{H}$	$\left(\frac{[H]_1}{[H]_0}\right) \exp\left(\frac{v - v_\mathrm{ATP}}{v_\mathrm{T}}\right)$
Na^+-Ca^{2+} exchanger	Na^+ Ca^{2+}	3 1	0 1	1 0	-1 1	$\Delta G_\mathrm{Na} = -3\mathrm{q}(v_\mathrm{Na} - v)$ $\Delta G_\mathrm{Ca} = 2\mathrm{q}(v_\mathrm{Ca} - v)$	-1	$2v_\mathrm{Ca} - 3v_\mathrm{Na}$	$\left(\frac{[\mathrm{Na}]_1}{[\mathrm{Na}]_0}\right)^3 \left(\frac{[\mathrm{Ca}]_0}{[\mathrm{Ca}]_1}\right) \exp\left(-\frac{v}{v_\mathrm{T}}\right)$
Na^+-I^- symporter	Na^+ I^{-1}	2 1	0 0	1 1	-1 -1	$\Delta G_\mathrm{Na} = -2\mathrm{q}(v_\mathrm{Na} - v)$ $\Delta G_\mathrm{I} = -\mathrm{q}(v_\mathrm{I} - v)$	-1	$-v_\mathrm{I} - 2v_\mathrm{Na}$	$\left(\frac{[\mathrm{Na}]_1}{[\mathrm{Na}]_0}\right)^2 \left(\frac{[\mathrm{I}]_1}{[\mathrm{I}]_0}\right) \exp\left(-\frac{v}{v_\mathrm{T}}\right)$
Na^+-H^+ exchanger	Na^+ H^+	1 1	0 1	1 0	-1 1	$\Delta G_\mathrm{Na} = -\mathrm{q}(v_\mathrm{Na} - v)$ $\Delta G_\mathrm{H} = \mathrm{q}(v_\mathrm{H} - v)$	0	$v_\mathrm{H} - v_\mathrm{Na}$	$\left(\frac{[\mathrm{H}]_1}{[\mathrm{H}]_0}\right) \left(\frac{[\mathrm{Na}]_0}{[\mathrm{Na}]_1}\right)$
K^+-Cl^- symporter	K^+ Cl^-	1 1	1 1	0 0	1 1	$\Delta G_\mathrm{K} = \mathrm{q}(v_\mathrm{K} - v)$ $\Delta G_\mathrm{Cl} = -\mathrm{q}(v_\mathrm{Cl} - v)$	0	$v_\mathrm{K} - v_\mathrm{Cl}$	$\left(\frac{[\mathrm{K}]_1}{[\mathrm{K}]_0}\right) \left(\frac{[\mathrm{Cl}]_1}{[\mathrm{Cl}]_0}\right)$
Na^+-K^+-Cl^- symporter	Na^+ K^+ Cl^-	1 1 2	0 0 0	1 1 1	-1 -1 -1	$\Delta G_\mathrm{Na} = -\mathrm{q}(v_\mathrm{Na} - v)$ $\Delta G_\mathrm{K} = -\mathrm{q}(v_\mathrm{K} - v)$ $\Delta G_\mathrm{Cl} = 2\mathrm{q}(v_\mathrm{Cl} - v)$	0	$2v_\mathrm{Cl} - v_\mathrm{Na} - v_\mathrm{K}$	$\left(\frac{[\mathrm{Na}]_0}{[\mathrm{Na}]_1}\right) \left(\frac{[\mathrm{K}]_0}{[\mathrm{K}]_1}\right) \left(\frac{[\mathrm{Cl}]_1}{[\mathrm{Cl}]_0}\right)^2$

Explicitly, combining equations (6) and (14), the flux rate resulting from simultaneously transporting molecules of m types across the membrane is

$$\begin{aligned} \alpha - \beta \quad = \quad & r \left[\prod_{s=1}^{m} \left(\frac{[C_s]_0}{[C_s]_1} \right)^{b n_s (d_s - c_s)} \exp\left(b \frac{\eta v - \delta_\mathrm{Extra} v_\mathrm{Extra}}{v_\mathrm{T}} \right) \right. \\ & \left. - \prod_{s=1}^{m} \left(\frac{[C_s]_0}{[C_s]_1} \right)^{(b-1) n_s (d_s - c_s)} \exp\left((b-1) \frac{\eta v - \delta_\mathrm{Extra} v_\mathrm{Extra}}{v_\mathrm{T}} \right) \right], \end{aligned} \tag{18}$$

which reads

$$\alpha - \beta = r \left\{ \exp\left[b \left(\frac{\eta v - v_o}{v_\mathrm{T}} \right) \right] - \exp\left[(b-1) \left(\frac{\eta v - v_o}{v_\mathrm{T}} \right) \right] \right\}, \tag{19}$$

when only ions are involved in the transport. The first, more complex, form of the flux in equation (18) could be useful when working with models in which the concentrations of different molecules are relevant.

Transmembrane current. Transport is electrogenic when the net charge transported is not zero ($\eta \neq 0$). In that case, the fluxes in equations (18) and (19) can be converted to a current density after multiplication by $\mathrm{q}\eta$. In short form,

$$i = \mathrm{q}\eta\,(\alpha - \beta) \tag{20}$$

with $\mathrm{q}r$ in amperes/m^2 or equivalent units.

Substitution of equation (18) or (19) into equation (20) yields general formula for the current generated by transmembrane ionic flux (Fig. 2), at a crossing location in the membrane, whether it is mediated by a single channel or pump. Recall that equation (20) can also be written explicitly in terms of the transmembrane concentrations of one or more of the ions involved using equation (18).

2.5 Special cases and examples

Expressions for current already present in the literature can be obtained from equation (20). Examples include electrodiffusive currents that result from integration of the Nernst-Planck equation along the length

PeerJ Preprints | https://doi.org/10.7287/peerj.preprints.1312v8 | CC BY 4.0 Open Access | rec: 16 Apr 2018, publ: 16 Apr 2018

of membrane pore (Johnston et al., 1995; **?**; **?**). Of particular interest, conductance-based currents are linear approximations of the formulation (20), around the reversal potential for the current. This explains why the Hodgkin and Huxley (1952) model captures many of the defining features of action potential generation, in spite of modeling the currents created by ion fluxes as resistive.

A number of nontrivial and important properties of transmembrane ionic currents, including rectification, are also described by equation (20). Examples of applications and special cases involving the formula (20) are shown next.

2.5.1 Rectifying and non-rectifying current

The flux of molecules across the membrane can be biased in either the outward or the inward direction. This was first called "anomalous rectification" by Katz (1949), who noticed that K^+ flows through muscle membranes more easily in the inward, than in the outward direction (Armstrong and Binstock, 1965; **?**). It was later found some K^+ channels display the bias in the opposite direction (**?**). The former type of K^+ current rectification is called inward, and the latter outward. Rectification is thus a bias in either of the two directions of transport, and it can be described by equation (18) when the value of b is moved away from 1/2. Rectification becomes more pronounced as b is closer to either 0 or 1, values that represent biases in the transport toward the source, or the target compartment, respectively. Another way to think about it is that values of b closer to 0 limit the flux when $\Delta G < 0$, and values of b closer to 1 limit the flux for $\Delta G > 0$ (Fig. 2). As a consequence, rectification yields an asymmetry in the graph of $\alpha - \beta$ as a function of ΔG (Fig. 2).

For electrogenic transport, the type of rectification (inward or outward) depends on what ions are being transported, and in what direction. In this case, rectification can be thought of as an asymmetric relationship between current flow and voltage, with respect to the reversal potential v_o. The particular case $b = 1/2$ (non rectifying) yields a functional form similar to that proposed by **?**, and later reproduced by (Endresen et al., 2000), namely

$$i = 2\mathrm{q}\eta r \sinh\left(\frac{\eta v - v_o}{2v_\mathrm{T}}\right). \tag{21}$$

From here on, subscripts will be used to represent different transport mechanisms. For instance, the current for a Na-Ca pump will be written as i_{NaCa}.

Electrodiffusion of K^+ through channels ($\eta = 1$ and $v_o = v_\mathrm{K}$), is outward for $v > v_\mathrm{K}$, and inward for $v < v_\mathrm{K}$. The K^+ current through the open pore is therefore

$$i_\mathrm{K} = \mathrm{q}r_\mathrm{K}\left\{\exp\left[b_\mathrm{K}\left(\frac{v - v_K}{v_\mathrm{T}}\right)\right] - \exp\left[(b_\mathrm{K} - 1)\left(\frac{v - v_K}{v_\mathrm{T}}\right)\right]\right\}. \tag{22}$$

Current flow through inward rectifier channels (Riedelsberger et al., 2015) can be fit to values of $b_\mathrm{K} < 1/2$. For instance,

$$i_{\mathrm{K}in} = \mathrm{q}r_\mathrm{K}\left[1 - \exp\left(\frac{v_\mathrm{K} - v}{v_\mathrm{T}}\right)\right], \quad (b_\mathrm{K} = 0), \tag{23}$$

describes a current with limited flow of K^+ in the outward direction, similar to the currents described originally by Katz (1949). Analogously, $b_\mathrm{K} > 1/2$ limits the inward flow. For example, the current

$$i_{\mathrm{K}out} = \mathrm{q}r_\mathrm{K}\left[\exp\left(\frac{v - v_\mathrm{K}}{v_\mathrm{T}}\right) - 1\right], \quad (b_\mathrm{K} = 1), \tag{24}$$

describes outward rectification (Riedelsberger et al., 2015).

Based on the work of Riedelsberger et al. (2015) on K^+ channels, the parameter b_K can be thought of as shifting the location of the S4 segment in K^+ channels to in the inner ($b_\mathrm{K} < 1/2$) or the outer portion of the membrane ($b_\mathrm{K} > 1/2$), respectively.

PeerJ Preprints | https://doi.org/10.7287/peerj.preprints.1312v8 | CC BY 4.0 Open Access | rec: 16 Apr 2018, publ: 16 Apr 2018

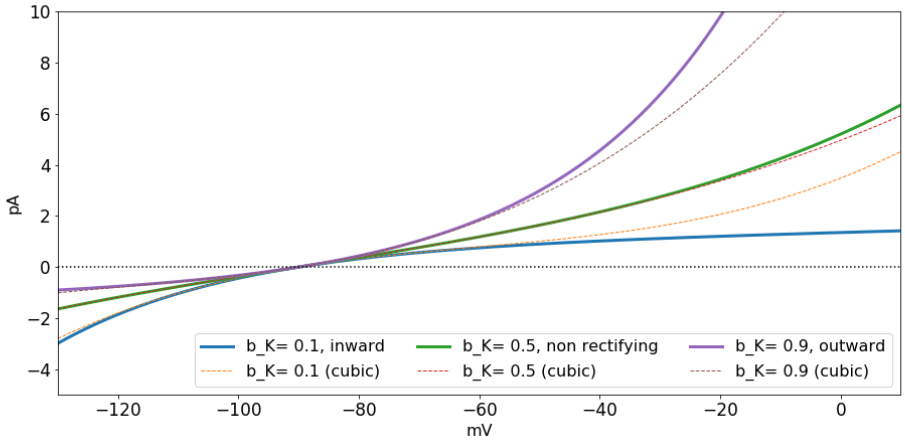

Figure 2: Fluxes for K-electrodiffusion for $b_{\rm K} \in \{0.1, 0.5, 0.9\}$ and their cubic approximations. Inward rectification occurs for $b_K < 1/2$ and outward rectification for $b_{\rm K} > 1/2$ and $\mathrm{q} r_{\rm K} N_{\rm K} = 1$.

2.5.2 Primary active transport.

The **Na-K ATPase** is a primary active transporter that uses the energy from the hydrolysis of one molecule of ATP for the uphill transport of Na^+ and K^+ (Weer et al., 1988). The kinetics of the **Na-K ATPase** can be assumed to translocate 3 Na^+ ions outward and 2 K^+ ions inward ($\eta_{\rm NaK} = 1$) with a reversal potential $v_{\rm NaK} = v_{\rm ATP} + 3v_{\rm Na} - 2v_{\rm K}$ (see Table 1) in a single transport event (Chapman, 1973; Gadsby et al., 1985; Garrahan and Glynn, 1967; Post and Jolly, 1957). Importantly, the transport kinetics of the Na-K ATPase and by extension, the current, reverse for potentials smaller than $v_{\rm NaK}$ (Weer et al., 1988).

The current-voltage relationships recorded from Na-K ATPases in guinea pig ventricular cells are shaped as hyperbolic sines (Gadsby et al., 1985). Those currents would be fit with $b_{\rm NaK}$ ≈1/2, yielding currents of the form

$$i_{\rm NaK}(v) \quad = \quad 2\mathrm{q} r_{\rm NaK} \sinh\left(\frac{v - v_{\rm NaK}}{2v_T}\right). \tag{25}$$

The voltage-dependence of the Na-K ATPase currents is reported to approach a plateau as v increases past the reversal potential for the current in response to steroids like strophandin (Nakao and Gadsby, 1989). In such cases, the Na-K ATPase current can be assumed to be inwardly rectifying and fit with values of $b_{\rm NaK} \approx 0$, so that,

$$i_{\rm NaK}(v) \quad = \quad \mathrm{q} r_{\rm NaK}\left[1 - \exp\left(\frac{v_{\rm ATP} + 3v_{\rm Na} - 2v_{\rm K} - v}{v_{\rm T}}\right)\right], \tag{26}$$

or alternatively,

$$i_{\rm NaK}(v) \quad = \quad \mathrm{q} r_{\rm NaK}\left[1 - \left(\frac{[\mathrm{Na}]_0}{[\mathrm{Na}]_1}\right)^3 \left(\frac{[\mathrm{K}]_1}{[\mathrm{K}]_0}\right)^2 \exp\left(\frac{v_{\rm ATP} - v}{v_{\rm T}}\right)\right]. \tag{27}$$

The rectification for the Na-K pump ATPase has also been reported to occur in small neurons of the dorsal root ganglion in rats (Hamada et al., 2003). The alternative expression (27) also explains qualitatively different behaviors of the Na-K current as a function of the transmembrane concentrations of Na^+ and K^+.

PeerJ Preprints | https://doi.org/10.7287/peerj.preprints.1312v8 | CC BY 4.0 Open Access | rec: 16 Apr 2018, publ: 16 Apr 2018

For instance, if either $[\mathrm{Na}]_1$ or $[\mathrm{K}]_0$ increase and $v > v_{\mathrm{NaK}}$, then the amplitude of i_{NaK} would increase, but at a smaller rate of change in comparison to when $v < v_{\mathrm{NaK}}$, which grows exponentially in size. This is also in line with reports of non significant changes in the transport by Na-K ATPases in response to elevated intracellular Na^+ during heart failure (Despa et al., 2002).

2.5.3 Secondary active transport.

An example of a pump that mediates secondary active transport is the *Na-Ca exchanger*, which takes 3 Na^+ ions from the extracellular compartment in exchange for one intracellular Ca^{2+} ion, in forward mode (Pitts, 1979; Reeves and Hale, 1984). The reversal potential for the current is $v_{\mathrm{NaCa}} = 2v_{\mathrm{Ca}} - 3v_{\mathrm{Na}}$, with $\eta_{\mathrm{NaCa}} = 1$. Assuming $b_{\mathrm{NaCa}} = 1/2$ gives

$$i_{\mathrm{NaCa}}(v) \quad = \quad 2\mathrm{q}r_{\mathrm{NaCa}} \sinh\left(\frac{v - v_{\mathrm{NaCa}}}{2v_T}\right) \tag{28}$$

The driving force $v - v_{\mathrm{NaCa}}$ could reverse in sign if the intracellular concentration of Ca^{2+}, or if the membrane potential increases enough. As a result, the current could have a dual contribution to the change in transmembrane potential, as predicted by some theoretical models of cardiac pacemaker activity (Rasmusson et al., 1990a,b).

2.5.4 Electrodiffusive transport

Consider transmembrane electrodiffusive transport of a single ionic type x, with z_x and v_x representing the valence and the Nernst potential for x-ions, respectively. In this case,

$$v_o = n_x(c_x - d_x)z_x v_x = \eta_x v_x,$$

and the generic expression (20) can be rewritten as

$$i_x(v) = \mathrm{q}\eta_x r_x \left\{\exp\left[\eta_x b_x \left(\frac{v - v_x}{v_T}\right)\right] - \exp\left[\eta_x (b_x - 1)\left(\frac{v - v_x}{v_T}\right)\right]\right\}. \tag{29}$$

In the absence of rectification ($b_x = 0.5$),

$$i_x(v) \quad = \quad 2\mathrm{q}\eta_x r_x \sinh\left(\eta_x \frac{v - v_x}{2v_T}\right). \tag{30}$$

For calcium channels,

$$i_{\mathrm{Ca}}(v) \quad = \quad 4\mathrm{q}r_{\mathrm{Ca}} \sinh\left(\frac{v - v_{\mathrm{Ca}}}{v_T}\right). \tag{31}$$

See **??** Table 1 for other examples.

2.5.5 Lower order approximations to the generic formulation and conductance based models

Conductance-based currents (Hodgkin and Huxley, 1952) are linear approximations of the generic current from equation (20), around the reversal potential v_o/η. To see this, rewrite the generic current from equation (20) as a series around v_o using Taylor's theorem so that

$$i \quad = \quad \mathrm{q}\eta r \left[\left(\frac{\eta v - v_o}{v_{\mathrm{T}}}\right) + \left(b - \frac{1}{2}\right)\left(\frac{\eta v - v_o}{v_{\mathrm{T}}}\right)^2 + \left(\frac{3b^2 - 3b + 1}{3!}\right)\left(\frac{\eta v - v_o}{v_{\mathrm{T}}}\right)^3 + \ldots\right]. \tag{32}$$

PeerJ Preprints | https://doi.org/10.7287/peerj.preprints.1312v8 | CC BY 4.0 Open Access | rec: 16 Apr 2018, publ: 16 Apr 2018

Truncation of the series to first order gives

$$i \approx g\left(v - \frac{v_o}{\eta}\right), \tag{33}$$

where $g = \eta^2 \mathrm{q} r / v_\mathrm{T}$ is in units of nS/μm^2, which is the form of the conductance-based current used in the Hodgkin and Huxley (1952) model. For instance, the linear approximation for the current through an open sodium channels around v_Na in equation (33) gives $g_\mathrm{Na} = \mathrm{q} r_\mathrm{Na} / v_\mathrm{T}$, and $v_o = \eta_\mathrm{Na} v_\mathrm{Na}$, with $\eta_\mathrm{Na} = -1$, so that $i_\mathrm{Na} \approx g_\mathrm{Na}(v - v_\mathrm{Na})$.

The applicability of the general formulations described above is illustrated next with models of cardiac and neuronal membrane potential.

3 Dynamics of transmembrane potential

To show the application of the general formulations discussed earlier, let us build a model of transmembrane potential dynamics with currents generated by N different electrogenic transport mechanisms. For simplification purposes, consider only one such mechanism, labeled as l, with $p_l N_l$ active sites, where N_l is the number of membrane sites where the lth transport mechanism is found, p_l is the proportion of such sites (might be voltage or ligand dependent). Then the total current mediated by the lth mechanism can be written as $a_l p_l \varphi_l(v)$ with $a_l = \mathrm{q} N_l r_l$ (in pA/μm^2), and

$$\varphi_l(v) = \exp\left[b_l\left(\frac{\eta_l v - v_l}{v_\mathrm{T}}\right)\right] - \exp\left[(b_l - 1)\left(\frac{\eta_l v - v_l}{v_\mathrm{T}}\right)\right]. \tag{34}$$

where v_l / eta_l is the reversal potential for the lth current, $l \in \{1, ..., N\}$. The transmembrane potential can then be assumed to change according to the equation

$$c_M \partial_t v = -\sum_{l=1}^{N} a_l p_l \varphi_l(v), \tag{35}$$

where c_M is a constant that describes the change in charge density around the membrane, as a function of v, in units of pF·μm^2 (Everitt and Haydon, 1968; Golowasch et al., 2009). An equivalent version of equation (35) can be obtained after multiplication of both sides by the membrane area, A. This may be convenient when trying to fit measurements of the membrane capacitance $C_M = A\, c_M$ taken directly from experimental recordings. The area can also be infered given C_M and c_M. A typical value for c_M is 0.01 pF/μm^2.

3.1 Cardiac pacemaking in the sinoatrial node

The pacemaking dynamics of cells in the rabbit sinonatrial node can be modeled with low dimensional dynamical systems based on K^+ and Ca^{2+} transmembrane transport (Herrera-Valdez, 2014; Herrera-Valdez and Lega, 2011) (Fig. 3). To do so, assume that transmembrane currents are mediated by electrodiffusion and pumping mechanisms: L-type Ca_{v13} channels (Mangoni et al., 2003), delayed-rectifier voltage-activated channels (Shibasaki, 1987), Na^+-Ca^{2+} exchangers, and Na^+-K^+ ATPases (Herrera-Valdez and Lega, 2011).

The temporal evolution of the system can then be described by equations of the form

$$C_M \partial_t v = -I_\mathrm{NaK}(v) - I_\mathrm{NaCa}(v, c) - I_\mathrm{Ca13}(v, w, c) - I_\mathrm{KD}(v, w), \tag{36}$$

where C_M is the membrane capacitance (pF), F is Faraday's constant (C/Mol), and k_c is a constant that controls the impact of the Ca^{2+} current on the free intracellular Ca^{2+} concentration. The proportion of

PeerJ Preprints | https://doi.org/10.7287/peerj.preprints.1312v8 | CC BY 4.0 Open Access | rec: 16 Apr 2018, publ: 16 Apr 2018

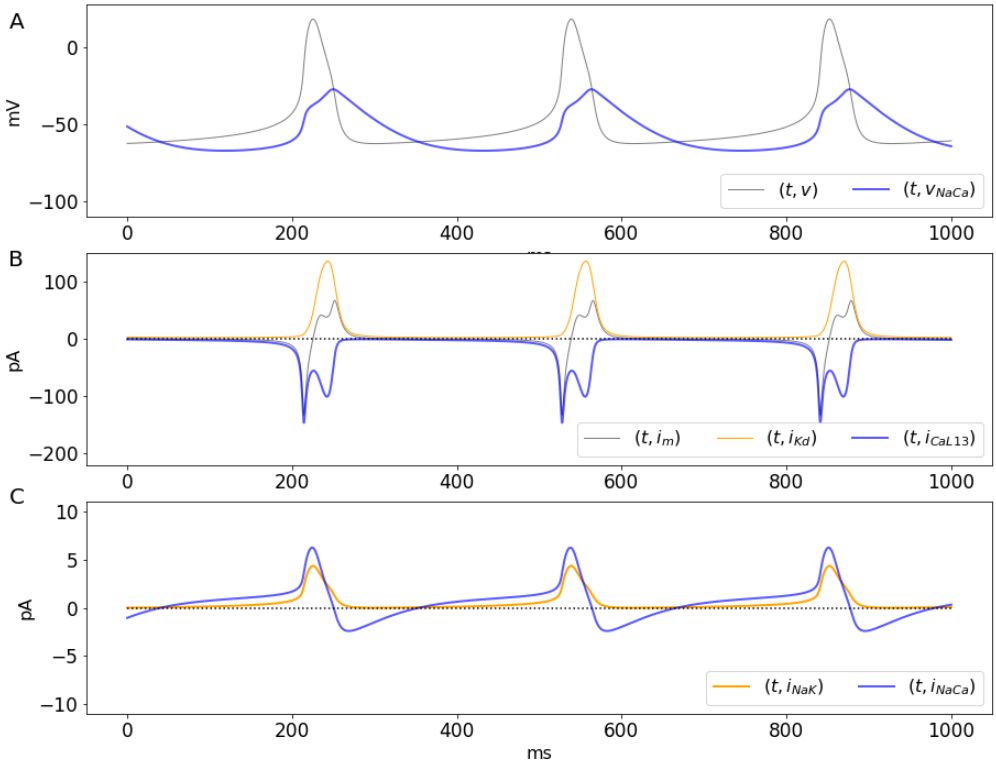

Figure 3: Central sinoatrial node pacemaking dynamics using the system (36)-(44). A. Transmembrane potential and the reversal potential v_{NaCa} as a function of time. B,C. Dynamics of large currents and small currents, respectively.

activated K^+ channels and the proportion of inactivated Ca^{2+} channels are both represented by a variable w (Av-Ron et al., 1991; Herrera-Valdez and Lega, 2011). The activation for the L-type Ca^{2+} channels is assumed to be at its voltage-dependent steady state (Herrera-Valdez and Lega, 2011). One important element to consider is that the activation phase of currents recorded in voltage-clamp experiments often displays sigmoidal time courses. Hodgkin and Huxley and others (**??**) have reported sigmoidally shaped whole cell currents in voltage-clamp as a function of time (see Fig. 3 in Hodgkin and Huxley, 1952), for some of the voltage commands, especially the ones for lower voltages. In line with the gating dynamics displayed in experiments like those described above, the activation and inactivation profiles of currents recorded in voltage-clamp can be described by solutions to equations from the family

$$\partial_t w = w\left[F_w(v) - w\right] R_w(v), \tag{37}$$

The change in the intracellular Ca^{2+} concentration can be modeled with a variable c exhibiting linear dynamics that in the absence of Ca^{2+} fluxes converge to a steady state c_∞, with increases proportional to the total transport of Ca^{2+} ions via L-type channels and Na^+-Ca^{2+} exchangers (Fig. 3).

$$\partial_t c = r_c\left(c_\infty - c\right) - \frac{k_c}{F}\left[I_{\mathrm{Ca}}(v,w) - I_{\mathrm{NaCa}}(v,c)\right]. \tag{38}$$

PeerJ Preprints | https://doi.org/10.7287/peerj.preprints.1312v8 | CC BY 4.0 Open Access | rec: 16 Apr 2018, publ: 16 Apr 2018

The transmembrane currents are given by

$$I_{\mathrm{NaK}}(v) = a_{\mathrm{NaK}}\,\varphi_{\mathrm{NaK}}(v), \tag{39}$$
$$I_{\mathrm{NaCa}}(v,c) = a_{\mathrm{NaCa}}\,\varphi_{\mathrm{NaCa}}(v,c), \tag{40}$$
$$I_{\mathrm{KD}}(v,w) = a_{\mathrm{KD}}\,w\,\varphi_{\mathrm{KD}}(v), \tag{41}$$
$$I_{\mathrm{Ca13}}(v,w,c) = a_{\mathrm{Ca13}T}\,(1-w)F_{m13}(v)\,\varphi_{\mathrm{Ca13}}(v,c), \tag{42}$$

with φ_x as defined above, for $x \in \{\mathrm{NaK}, \mathrm{NaCa}, \mathrm{KD}, \mathrm{Ca13}\}$. The steady state for the activation of voltage-dependent channels is described by the function

$$F_u(v) = \frac{exp\left(g_u \frac{v-v_u}{v_{\mathrm{T}}}\right)}{1+exp\left(g_u \frac{v-v_u}{v_{\mathrm{T}}}\right)}, \quad u \in \{m,w\} \tag{43}$$

which has a graph with sigmoidal shape as a function of v, with steepness controlled by g_u and a half-activation potential v_u, for $u \in \{m,w\}$. The activation rate for K^+ channels is a voltage-dependent function of the form

$$R_w(v) = r_w\left[exp\left(b_w g_w \frac{v-v_w}{v_{\mathrm{T}}}\right) + exp\left((b_w-1)g_w \frac{v-v_w}{v_{\mathrm{T}}}\right)\right]. \tag{44}$$

The parameter b_w represents a bias in the conformational change for activation. Values of b_w close to 0 represent a bias in favor of deactivation and b_w close to 1 a bias toward activation. Notice that the function R_w has the shape of a hyperbolic cosine when b_w is 1/2.

The solutions of equations (36)-(44) reproduce important features of the membrane dynamics observed in the rabbit's central sinoatrial node, including the period, amplitude, and maximum speed of the action potentials (Zhang et al., 2000). One interesting behavior that is shown in the solutions to the system is that the Na-Ca current reverses when $v = v_{\mathrm{NaCa}}$ (Fig. 3A, blue line). In this example, $v_{\mathrm{NaCa}} < v$ and $i_{\mathrm{NaCa}} > 0$ during the initial depolarization and until the maximum downstroke rate, approximately, which means extrusion by the Na-Ca exchanger occurs only for a brief period of time during the downstroke and the initial recovery after each action potential (Fig. 3C, blue line).

The time course of the Ca^{2+} current shows a partial inactivation with a double peak (Fig. 3B) around a local minimum, as previously reported in different studies involving spiking dynamics (Carter and Bean, 2009; Rasmusson et al., 1990a,b). The local minimum occurs at the peak of the action potential, as the total current passes through zero (Fig. 3B, linea gris). The double peak in the Ca^{2+} current is in agreement with data from voltage-clamp experiments (Mangoni et al., 2006). The Ca^{2+} channel inactivation presented here is also the activation of the K^+ channels (Herrera-Valdez and Lega, 2011), an assumption not present in other more complicated models that show the double activation of the L-type Ca^{2+} channels (Mitchell and Schaeffer, 2003). Such models include extra assumptions like a second activation variable, or the multiple terms in the steady state gating, or in the time constant for activation or inactivation (see Rasmusson et al., 1990a,b). That is not the case in the model presented here.

It is important to remark that the dual role played by w is not the cause of the double activation, since it can also happen for non-inactivating Ca^{2+} channels (Fig. 4A, linea gris). The double activation also happens in models in which activation of K^+ channels and inactivation of Ca^{2+} or Na^+ channels are represented by different variables (Rasmusson et al., 1990a) and in dynamic voltage clamp experiments on neurons in which there are transient and persistent sodium channels (Carter and Bean, 2009).

The first peak for the Ca^{2+} current occurs when v reaches the maximum depolarization rate (Fig. 4B). The Ca^{2+} current starts to decrease as w increases and until v reaches its maximum. After the peak of the pacemaking oscillation, the Ca^{2+} current increases again, reaching a second peak shortly before the K^+ current is maximally activated; that is, shortly before w reaches its highest value and the decrease in v is at its maximum too.

PeerJ Preprints | https://doi.org/10.7287/peerj.preprints.1312v8 | CC BY 4.0 Open Access | rec: 16 Apr 2018, publ: 16 Apr 2018

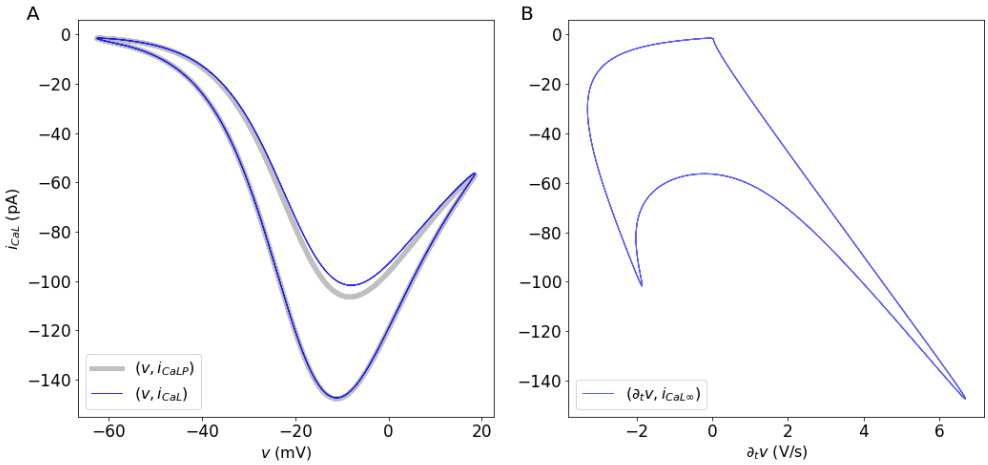

Figure 4: Calcium current dynamics and double activation. The joint behavior of the L-type Ca^{2+} current with respect to the transmembrane potential (A, blue line) and for non-inactivating channels (A, gray line), and with respect to the time-dependent change in v (B).

The double peak in the Ca^{2+} current is reflected in the intracellular Ca^{2+} current (Figure 5, gray line), and therefore, on the Nernst potential for Ca^{2+} (Figure 5, blue line), which displays two decreasing phases, the first and faster one during the initial activation of the L-type channels, and a second phase during the second peak of the Ca^{2+} current. By extension, the reversal potential for the Na-Ca exchanger, $v_{\mathrm{NaCa}} = 3v_{\mathrm{Na}} - 2v_{\mathrm{Ca}}$ (Figure 5, orange line) also has two phases, this time increasing, related to the two activations of the Ca^{2+} channels. Increases in the intracellular Ca^{2+} (Figure 5, gray line) concentration decrease the Nernst potential for Ca^{2+} and viceversa. By extension, the reversal potential for the Na-Ca exchanger, $v_{\mathrm{NaCa}} = 3v_{\mathrm{Na}} - 2v_{\mathrm{Ca}}$ increases if c increases. As already mentioned, Ca^{2+} enters the cell in exchange for Na^{+} that moves out during most of the action potential (Figure 5).

4 Discussion

A generic, macroscopic model for transmembrane fluxes has been derived by directly calculating the work required to transport molecules across the membrane. The derivation is based on a general thermodynamic scheme that takes into account the rate, stoichiometry, and the direction in which the molecules are transported across the membrane. These biophysical parameters are then combined to write expressions for directional fluxes based on van't Hoff (1884) and Arrhenius (1889) formulations, weighted as in the Butler/Erdey-Gruz/Volmer equation (Butler, 1924; Erdey-Grúz and Volmer, 1930). The result is a general description (equation 20) of the transmembrane molecular flux as a difference of exponential functions, each describing the transport dynamics in the "forward" and "backward" directions, relative to a source compartment. The two exponential functions depend on a common expression involving the transmembrane concentrations of the molecules being transported, and possibly the transmembrane potential.

Rectification in transmembrane currents mediated by channels is typically modeled modifying the dynamics of the gating variables of the current. The general formulas for transmembrane transport include a bias term b that controls the relative contribution of inward and outward components the transport. Hence, different types of rectification can be described by favoring one of the directions for transport,

PeerJ Preprints | https://doi.org/10.7287/peerj.preprints.1312v8 | CC BY 4.0 Open Access | rec: 16 Apr 2018, publ: 16 Apr 2018

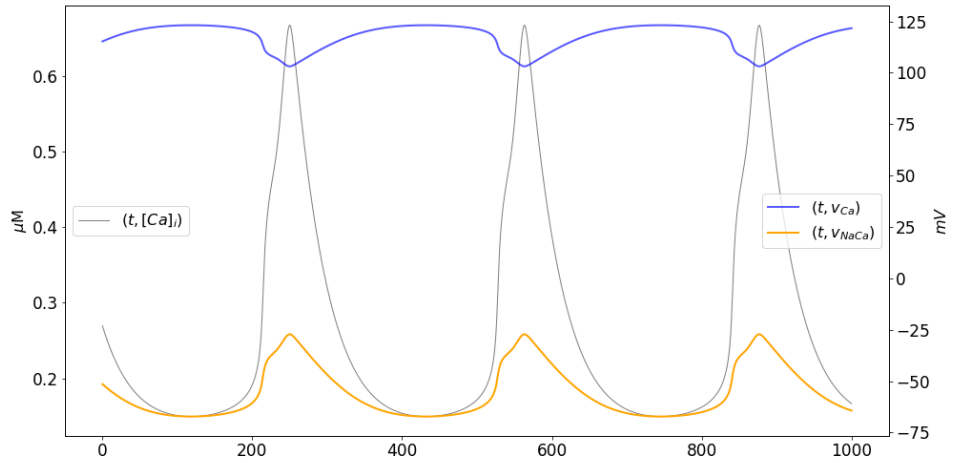

Figure 5: Calcium dynamics during pacemaking. Time courses of the intracellular calcium concentration (gray, left axis), the Nernst potential for Ca^{2+} (blue), and the reversal potential for the Na-Ca exchanger.

conceptually in line with the "anomalous rectification" originally reported by Katz (1949) for K^+ in muscle cells. It is important to remark that non-rectifying currents with $b = 1/2$ are nonlinear functions of ΔG, which shows that the nonlinearity of the current-voltage relationships is not the defining characteristic of rectification; as argued in some textbooks (see Kew and Davies, 2010). It is also important to note that the bias term is not part of any gating mechanism. Based on the work of Riedelsberger et al. (2015), the inward (outward, respectively) rectification in K^+ channels corresponds to a bias in the location of the fourth transmembrane segment of the channel (S4) toward the intracellular (extracellular) portion of the membrane (Riedelsberger et al., 2015). Therefore, the rectification term can be thought of as representing a structural component of the transmembrane protein through which molecules move (Fig. 2). Outward rectification in K^+ channels can be explained, for instance, by biasing the flux of K^+ the forward (outward) direction ($b_K > 1/2$). Instead, inward rectification can be obtained by biasing the transport in the backward (inward) direction ($b_K < 1/2$).

The formulation for transmembrane flux may be rewritten in different alternative forms that can be found throughout the literature (see equations (18) and (19), Goldman, 1943; Johnston et al., 1995) that can be useful for numerical calculations involving the concentrations of molecules of interest, like the available ATP. Of particular interest, the widely used conductance-based models for current from the seminal work of Hodgkin and Huxley (1952) turn out to be linear approximations of the generic current described here (Herrera-Valdez, 2012). It can also be shown that electrodiffusive transmembrane currents derived from the Nernst-Planck equation (Nernst, 1888; Planck, 1890), turn out particular cases of the generic formulation presented here (see also Herrera-Valdez, 2014, for details). Examples include the constant field approximation (Clay et al., 2008; Hille, 1992; Johnston et al., 1995), the non-rectifying currents proposed by Endresen et al. (2000), and more general electrodiffusive currents that includes a bias term accounting for rectification (Herrera-Valdez, 2014; Johnston et al., 1995). Of possible interest to mathematicians working on bifurcation theory, a third order approximation (equation (32)) resembling the Fitz-Hugh equations (Fitz-Hugh, 1966; FitzHugh, 1955, 1961), can be used to construct models that give very close approximations to the full model, while keeping biophysical characteristics like rectification. Further, the third order approximation opens the possibility of expanding on the analysis of dynamical systems based on these generic formulas to study normal forms and bifurcations.

One question of interest because of its possible impact on the interpretation of results from existing

PeerJ Preprints | https://doi.org/10.7287/peerj.preprints.1312v8 | CC BY 4.0 Open Access | rec: 16 Apr 2018, publ: 16 Apr 2018

Table 2: Parameters for the cardiac SAN pacemaker model.

Parameter	Value	Units	Description
C_M	20	pF	Membrane capacitance
a_{Ca}	1	pA	Maximum amplitude for the L-type Ca^{2+} current
a_{K}	700	pA	Maximum amplitude for the K^+ current
a_{NaK}	1	pA	Maximum amplitude for the Na^+-K^+ current
a_{NaCa}	2.5	pA	Maximum amplitude for the Na^+-Ca^{2+} current
v_{ATP}	-420	mV	Potential ATP hydrolysis
v_{Na}	60	mV	Nernst potential for Na^+
v_{K}	-89	mV	Nernst potential for K^+
$v_{\mathrm{NaK}} = 3v_{Na} - 2v_{\mathrm{K}} + v_{\mathrm{ATP}}$	-62	mV	Reversal potential for the for Na^+-K^+ ATPase current
$v_{\mathrm{NaCa}} = 2v_{\mathrm{Ca}} - 3v_{\mathrm{Na}}$	–	mV	Reversal potential for the for Na^+-Ca^{2+} current (v_{Ca} depends continuously on $[Ca]_i$)
v_{m13}	-17	mV	Half-activation potential for Ca_{v13} L-type Ca^{2+}-current
v_w	0	mV	Half-activation potential for the transient K^+-current
g_{m13}	4	–	Activation slope factor for the Ca_{v13} L-type Ca^{2+}-current
g_w	3	–	Activation slope factor for the K^+-current
r_w	0.07	s^{-1}	Activation rate for the cardiocyte K^+-current
b_w	0.35	–	Activation slope factor for the K^+-current
b_{NaK}	0.5	–	Non-rectification bias for the Na^+-K^+-current
b_{K}	0.5	–	Rectification for the transient K^+-current
b_{Na}	0.5	–	Non-rectification bias for the transient Na^+-current
b_{Ca}	0.5	–	Non-rectification bias for the Ca_{v13} L-type Ca^{2+}-current
c_∞	0.1	μM	Minimal (resting) intracellular Ca^{2+}-concentration
r_c	0.02	ms^{-1}	Ca^{2+} removal rate
k_c	2	–	Conversion factor between Ca^{2+} current and intracellular Ca^{2+} concentration

modeling studies, how does the excitability and the resulting dynamics in a model of membrane dynamics change when using the thermodynamic transmembrane currents or their approximations? The question has been addressed in a study in which two simple neuronal models with currents mediated by Na^+ and K^+, each equipped with the same biophysical gating properties and the same relative contributions for the currents, but one with currents as in equation (21), the other with conductance-based currents. The two models display a number of qualitative and quantitative differences worth considering for the choice of a model in future theoretical studies (Herrera-Valdez, 2012). For a start, the two models are not topologically equivalent across many ratios of the relative contributions of K^+ and Na^+ channels (Herrera-Valdez, 2012); as would be expected by the fact that conductance-based formulations are only linear approximations of the generic currents. One of the most notable differences is the contribution of the nonlinear, high order terms from (20), which results in more realistic upstrokes for action potentials and an overall increased excitability; in this case characterized in terms of the minimum sustained current necessary to produce at least one action potential. The increased excitability of the membrane is due, in part, to the large, exponential contribution of the Na^+ and Ca^{2+} channels to the change in the transmembrane potential

PeerJ Preprints | https://doi.org/10.7287/peerj.preprints.1312v8 | CC BY 4.0 Open Access | rec: 16 Apr 2018, publ: 16 Apr 2018

near rest. The time course of the Na^+ current during the upstroke of the action potential with the generic model is much sharper than that of the conductance-based formulation, resulting in a faster upstroke of the action potential; and in better agreement with observations in cortex and other tissues (Naundorf et al., 2006). It is important to remark that the sharper increase in the change of the membrane potential is a consequence of the nonlinear driving force terms of the current (the flux term in the generic formulation) and not in the activation dynamics for the transient Na^+ current.

The generic formulation for both passive and active transmembrane transport can be thought of as a recipe to build a toolbox that facilitates the construction and analysis of models of membrane potential dynamics. The generality and versatility of the thermodynamic transmembrane transport formulations is illustrated with a model of the dynamics of cardiac pacemaking (equations (36)-(44)); another example with a model for a fast spiking interneuron can be found in the appendix A. The ion fluxes in the model are assumed to be mediated by two different types of voltage-gated channels and two different types of pumps, all represented with the *same* functional form (see DiFrancesco and Noble (1985); Herrera-Valdez and Lega (2011); Rasmusson et al. (1990b) for examples in which that is not the case).

One important advantage of the generic formulation is that it includes the possibility of explicitly estimating the number of channels or pumps mediating each of the transport mechanisms of interest. This has proven to be useful to study the relative contributions of different currents to the excitability of neurons (see Appendix A and Herrera-Valdez et al., 2013), cardiocytes (Herrera-Valdez, 2014), and other different tissues (unpublished work). Another extension of possible interest to study physiological processes within single cells is that of modelling the transmembrane transport between organelles and the cytosolic compartment, which can be done by directly replacing the difference $c_s - d_s$ in equation (7) with 1 or -1, accounting for the direction of transmembrane motion of molecules relative to the outer compartment. This and other generalizations enable the possibility of studying the interdependence between electrical excitability across tissues and animal species (Herrera-Valdez et al., 2013), and its cross-interactions with metabolism and other processes of physiological importance, all from a general theoretical framework with common formulations.

Implications for experimentalists. One of the main advantages of the generic expressions is that fits to ionic currents can be made straight from the voltage-clamp data without much effort, and without having to calculate conductances, which amounts to imposing the assumption that the current to voltage relationship is linear. Fits to experimental currents can then be directly put into equations describing the change in the membrane potential, and model membrane dynamics of interest without having to make many extra adjustments, as it is the case for most conductance-based models restricted to data. As mentioned above, the idea of a "maximal conductance" is not quite as correct as the "maximal current" in the models presented in previous sections (see Table 2 and section on linear approximations), in part because of the inherent nonlinearity of the flux.

The model for current in equation (21) has been used to construct simplified models for the membrane dynamics of different cell types, including motor neurons in *Drosophila melanogaster* (Herrera-Valdez et al., 2013), pyramidal cells in the young and ageing hippocampus of rats (McKiernan et al., 2015), medium spiny neurons in the mouse striatum (Suárez et al., 2015), rabbit sinoatrial node cells (Herrera-Valdez, 2014), and other types of excitable cells (McKiernan and Herrera-Valdez, 2012). In all cases the models were adjusted with experimental data.

In sum, the theoretical descriptions of transmembrane transport derived and presented here provide a unifying framework to model passive and active transmembrane transport, and make predictions that can be tested experimentally (Shou et al., 2015).

PeerJ Preprints | https://doi.org/10.7287/peerj.preprints.1312v8 | CC BY 4.0 Open Access | rec: 16 Apr 2018, publ: 16 Apr 2018

5 Acknowledgments

The author wishes to thank Joceline Lega, Timothy Secomb, and Raphael Gruener at the University of Arizona; and José Bargas Díaz and Antonio Laville from the Cellular Physiology Institute at UNAM for all the time spent in discussions that helped to solidify and deepen the ideas presented in this paper.

Table A1: Physical constants. The conversion factor f from pA to $\mu M \cdot ms^{-1} = mM \cdot s^{-1}$ implies $\Rightarrow M = f \cdot 10^{-9}$ Coul. Then $f = 10^9$ M/Coul = $10^9 \cdot 96485.3329/F \approx 10^{14}$ M/Coul.

Constant	Value	Units	Description
T_0	273.16	degrees Kelvin	Zero absolute temperature
N_A	6.023 $\times$ 10^{23}	molecules/Mole	Avogadro's number
q	1.60217733 $\times 10^{-19}$	Coulombs/molecule	Elementary charge (electrical charge on the electron)
k	1.381 $\times 10^{-23}$	Joules/^{o}Kelvin	Boltzmann constant
	8.62 $\times 10^{-5}$	eV/ ^{o}Kelvin	
$\mathrm{F} = \mathrm{q}N_A$	96485.33289	Coulombs/Mole	Faraday's constant (the magnitude of electric charge per mole of electrons)
$\mathrm{R} = \mathrm{k}N_A$	1.987	cal/(Mole ^{o}Kelvin)	Gas constant

A Fast spiking interneuron dynamics

A simple model of the dynamics of a fast spiking (FS) striatal interneuron can be constructed using (35). To do so, assume the transmembrane potential depends on three currents respectively mediated by Na-K pumps, non-inactivating K^+ channels, and Na^+ channels with transient dynamics, with voltage-dependent gating in both channels. It is also assumed that the proportion of activated K^+ is represented by a variable $w \in [0, 1]$, which also represents the proportion of inactivated Na^+ channels (Av-Ron et al., 1991; Rinzel, 1985). That is, $1 - w$ represents the proportion of non-inactivated Na^+ channels. The dynamics for w can be assumed to follow a logistic scheme, capturing the behaviour of delayed-rectifier K^+ currents typically recorded in voltage clamp mode without adding extra powers to w (see for instance Hodgkin and Huxley, 1952, and the Appendix). It is also assumed that sodium channel activation is fast, described by its steady state function of v.

PeerJ Preprints | https://doi.org/10.7287/peerj.preprints.1312v8 | CC BY 4.0 Open Access | rec: 16 Apr 2018, publ: 16 Apr 2018

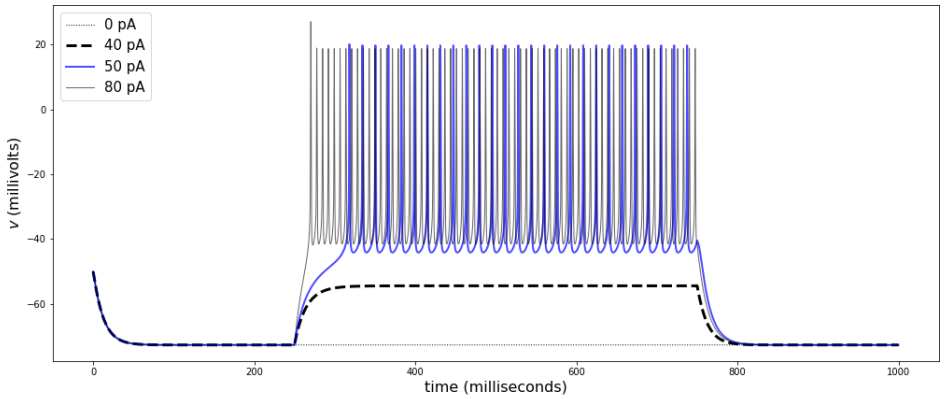

Figure A1: Rest to spiking transitions of FS interneuron under current clamp. The traces show responses to current-clamp stimulation of different amplitudes. The transition between rest and spiking with a rheobase occurs between 40 and 50 pA, as shown for some FS neurons in the mouse striatum (Orduz et al., 2013). The traces correspond to stimulation amplitudes of 0 (gray dots), 40 (black dashed line), 50 (blue), and 80 pA (gray). Parameters can be found in Table A2.

Explicitly, the dynamics of the system can then be captured by coupled differential equations of the form

$$C_m \partial_t v = -(1-w) F_m(v) A_{\mathrm{NaT}}\, \psi_{\mathrm{NaT}}(v) - w A_{\mathrm{KaD}}\, \psi_{\mathrm{KaD}}(v) - A_{\mathrm{NaK}}\, \psi_{\mathrm{NaK}}(v), \quad \text{(A1)}$$

$$\partial_t w = w\,[F_w(v) - w]\, R_w(v), \quad \text{(A2)}$$

where

$$F_u(v) = \frac{exp\left(g_u \frac{v-v_u}{v_{\mathrm{T}}}\right)}{1 + exp\left(g_u \frac{v-v_u}{v_{\mathrm{T}}}\right)}, \quad u \in \{m, w\} \quad \text{(A3)}$$

is a function with sigmoidal shape that represents the steady state activation of the gating variables m and w, respectively, and has sigmoidal shape as a function of v. The parameter g_u controls the steepness of the steady state as a function of v. The activation rate for K^+ channels depends is a voltage-dependent function

$$R_w(v) = r_w \left[exp\left((b_w - 1) g_w \frac{v - v_w}{v_{\mathrm{T}}}\right) + exp\left(b_w g_w \frac{v - v_w}{v_{\mathrm{T}}}\right)\right]. \quad \text{(A4)}$$

The parameter b_w represents a bias in the conformational change for activation. Values of b_w close to 0 represent a rate of activation that is voltage-dependent with voltage-independent de-activation. In contrast, b_w close to 1 represents voltage-dependent de-activation, and a voltage-independent activation, respectively. Notice that the function R_w has the shape of a hyperbolic cosine when b_w is 1/2.

The functions in equation (A2) can be derived by considering the work required for voltage-dependent gating, as previously described by Willms et al. (1999), Endresen et al. (2000), and Herrera-Valdez et al. (2013), among others.

The dynamics of the system are such that, as v increases, w increases, but at a slower rate in comparison to v. This is because the activation w is always moving toward its steady state value, which

PeerJ Preprints | https://doi.org/10.7287/peerj.preprints.1312v8 | CC BY 4.0 Open Access | rec: 16 Apr 2018, publ: 16 Apr 2018

increases as v increases. Once w increases, the Na^+ current tends to decrease and the K^+ current tends to increase, thereby causing a decrease in v. The slower dynamics in w relative to those in v capture the delay between the amplification caused by the Na^+ current and the recovery caused by the K^+ current. The current mediated by Na/K-ATPase acts as an extra attracting force toward v_{NaK} that increases nonlinearly as the distance between v and v_{NaK} increases.

Striatal FS interneurons display maximum $\partial_t v$ between 100 and 200 V/s. In current clamp mode, most neurons are silent, and show transitions between rest and repetitive spiking at a rheobase current of approximately 90 pA, with initial firing rates between 50 and 60 Hz and a delay to first spike in the transition that decreases as the stimulus amplitude increases (Fig.A1, parameters in Table A2).

To include these properties into the model, the membrane capacitance was specified first, then the maximum $\partial_t v$ was adjusted by fitting the parameter a_{NaT}, and then the contributions for the K^+ channels and the Na-K ATPase are set to obtain spiking and fit the rheobase.

The model in equations (A1)-(A4) reproduces dynamics observable in fast spiking neurons in CA1 (Erisir et al., 1999) or in the striatum (Orduz et al., 2013; Tepper et al., 2010).

Table A2: Parameters for the fast spiking interneuron model.

Parameter	Value	Units	Description
Current amplitudes and capacitance for the neuronal membrane model			
C_m	30	pF	Membrane capacitance
$\bar{a}_{\mathrm{NaK}}$	67	pA	Maximum amplitude for the Na^+-K^+ ATPase current
$\bar{a}_{\mathrm{K}}$	4400	pA	Maximum amplitude for the delayed-rectifier K^+ current
$\bar{a}_{\mathrm{Na}}$	1400	pA	Maximum amplitude for the transient Na^+ current
v_{ATP}	-430	mV	Potential ATP hydrolysis
$v_{\mathrm{NaK}} = 3v_{Na} - 2v_{\mathrm{K}} + v_{\mathrm{ATP}}$	-72	mV	Reversal potential for the for Na^+-K^+ ATPase current
v_{K}	-89	mV	Nernst potential for K^+
v_{Na}	60	mV	Nernst potential for Na^+
v_{mT}	-17	mV	Half-activation potential for the transient Na^+-current
v_w	-5	mV	Half-activation potential for the transient K^+-current
g_{mT}	5	–	Activation slope factor for the transient Na^+-current
g_w	4	–	Activation slope factor for the K^+-current
r_w	2	s^{-1}	Activation rate for the neuronal K^+-current
b_w	0.3	–	Activation slope factor for the K^+-current
b_{NaK}	0.5	–	Non-rectification for the Na^+-K^+-current
b_{K}	0.5	–	Non-rectification for the transient K^+-current
b_{Na}	0.5	–	Non-rectification for the transient Na^+-current

PeerJ Preprints | https://doi.org/10.7287/peerj.preprints.1312v8 | CC BY 4.0 Open Access | rec: 16 Apr 2018, publ: 16 Apr 2018

References

David J. Aidley. *The Physiology of Excitable Cells*. Cambridge University Press, 4 edition, 1998. ISBN 0521574153,9780521574150. URL http://gen.lib.rus.ec/book/index.php?md5=25AD083C33F37AC8E44F3CE90E3B3B84.

R. W. Aldrich, D. P. Corey , and C. F. Stevens. A reinterpretation of mammalian sodium channel gating based on single channel recording. *Nature*, 306(5942):436–441, 1983.

W. Almers and E. W. McCleskey. Non-selective conductance in calcium channels of frog muscle: calcium selectivity in a single-file pore. *The Journal of Physiology*, 353(1):585, 1984.

Clay M Armstrong and Leonard Binstock. Anomalous rectification in the squid giant axon injected with tetraethylammonium chloride. *The Journal of general physiology*, 48(5):859–872, 1965.

Svante Arrhenius. Über die reaktionsgeschwindigkeit bei der inversion von rohrzucker durch säuren. *Zeitschrift für physikalische Chemie*, 4(1):226–248, 1889.

E. Av-Ron, H. Parnas, and L. A. Segel. A minimal biophysical model for an excitable and oscillatory neuron. *Biological Cybernetics*, 65(6):487–500, 1991.

L. Barr. Membrane potential profiles and the Goldman equation. *Journal of Theoretical Biology*, 9(3): 351–356, 1965.

B. P. Bean and E. Rios. Nonlinear charge movement in mammalian cardiac ventricular cells. components from na and ca channel gating. *The Journal of general physiology*, 94(1):65, 1989.

H Stanley Bennett. The concepts of membrane flow and membrane vesiculation as mechanisms for active transport and ion pumping. *The Journal of biophysical and biochemical cytology*, 2(4):99, 1956.

M.P. Blaustein, J.P.Y. Kao, and D.R. Matteson. *Cellular physiology*. Elsevier/Mosby, 2004. ISBN 0323013414.

Andreas Blicher and Thomas Heimburg. Voltage-gated lipid ion channels. *PLoS One*, 8(6):e65707, 2013.

JAV Butler. Studies in heterogeneous equilibria. part 2.—the kinetic interpretation of the nernst theory of electromotive force. *Transactions of the Faraday Society*, 19(March):729–733, 1924.

Brett C Carter and Bruce P Bean. Sodium entry during action potentials of mammalian neurons: incomplete inactivation and reduced metabolic efficiency in fast-spiking neurons. *Neuron*, 64(6):898–909, 2009.

J Brian Chapman. On the reversibility of the sodium pump in dialyzed squid axons: A method for determining the free energy of atp breakdown? *The Journal of general physiology*, 62(5):643, 1973.

J. R. Clay, D. Paydarfar, and D. B. Forger. A simple modification of the hodgkin and huxley equations explains type 3 excitability in squid giant axons. *Journal of The Royal Society Interface*, 5(29):1421–1428, 2008.

K. S. Cole. Electrodiffusion models for the membrane of squid giant axon. *Physiological Reviews*, 45(2): 340, 1965. ISSN 0031-9333.

Sanda Despa, Mohammed A Islam, Christopher R Weber, Steven M Pogwizd, and Donald M Bers. Intracellular na+ concentration is elevated in heart failure but na/k pump function is unchanged. *Circulation*, 105(21):2543–2548, 2002.

PeerJ Preprints | https://doi.org/10.7287/peerj.preprints.1312v8 | CC BY 4.0 Open Access | rec: 16 Apr 2018, publ: 16 Apr 2018

A. Destexhe, Z. F. Mainen, and T. J. Sejnowski. An Efficient Method for Computing Synaptic Conductances Based on a Kinetic Model of Receptor Binding. *Neural Computation*, 6(1):14–18, 1994.

D. DiFrancesco and D. Noble. A model of cardiac electrical activity incorporating ionic pumps and concentration changes. *Philosophical Transactions of the Royal Society of London. Series B, Biological Sciences*, 307:353–398, 1985.

Declan A Doyle, Joao Morais Cabral, Richard A Pfuetzner, Anling Kuo, Jacqueline M Gulbis, Steven L Cohen, Brian T Chait, and Roderick MacKinnon. The structure of the potassium channel: molecular basis of k+ conduction and selectivity. *science*, 280(5360):69–77, 1998.

L. P. Endresen, K. Hall, J. S. Hoye, and J. Myrheim. A theory for the membrane potential of living cells. *European Journal of Biophysics*, 29:90–103, 2000.

Th Erdey-Grúz and M Volmer. Zur theorie der wasserstoff überspannung. *Zeitschrift für Physikalische Chemie*, 150(1):203–213, 1930.

A Erisir, D Lau, B Rudy, and CS Leonard. Function of specific k+ channels in sustained high-frequency firing of fast-spiking neocortical interneurons. *Journal of neurophysiology*, 82(5):2476–2489, 1999.

CT Everitt and DA Haydon. Electrical capacitance of a lipid membrane separating two aqueous phases. *Journal of theoretical biology*, 18(3):371–379, 1968.

Isabelle Favre, Edward Moczydlowski, and Laurent Schild. On the structural basis for ionic selectivity among na+, k+, and ca2+ in the voltage-gated sodium channel. *Biophysical journal*, 71(6):3110–3125, 1996.

Willy Feller. On the logistic law of growth and its empirical verifications in biology. *Acta biotheoretica*, 5(2): 51–66, 1940.

Richard Fitz-Hugh. *Mathematical models of excitation and propagation in nerve*. Publisher Unknown, 1966.

Richard FitzHugh. Mathematical models of threshold phenomena in the nerve membrane. *Bulletin of Mathematical Biology*, 17(4):257–278, 1955.

Richard FitzHugh. Impulses and physiological states in theoretical models of nerve membrane. *Biophysical journal*, 1(6):445–466, 1961.

Sidney Fleischer and Becca Fleischer. *ATP-Driven Pumps and Related Transport: Calcium, Proton, and Potassium Pumps*. Academic Press, 1988.

David C Gadsby, Junko Kimura, and Akinori Noma. Voltage dependence of na/k pump current in isolated heart cells. *Nature*, 315(6014):63–65, 1985.

D.C. Gadsby. Ion channels versus ion pumps: the principal difference, in principle. *Nature Reviews Molecular Cell Biology*, 10(5):344–352, 2009.

PJ Garrahan and IM Glynn. The behaviour of the sodium pump in red cells in the absence of external potassium. *The Journal of physiology*, 192(1):159–174, 1967.

D. E. Goldman. Potential, impedance, and rectification in membranes. *Journal of general Physiology*, 27 (1):37, 1943.

PeerJ Preprints | https://doi.org/10.7287/peerj.preprints.1312v8 | CC BY 4.0 Open Access | rec: 16 Apr 2018, publ: 16 Apr 2018

Jorge Golowasch, Gladis Thomas, Adam L Taylor, Arif Patel, Arlene Pineda, Christopher Khalil, and Farzan Nadim. Membrane capacitance measurements revisited: dependence of capacitance value on measurement method in nonisopotential neurons. *Journal of Neurophysiology*, 102(4):2161–2175, 2009.

B Gustafsson, Martin Galvan, Peter Grafe, and H Wigström. A transient outward current in a mammalian central neurone blocked by 4-aminopyridine. *Nature*, 299(5880):252, 1982.

David Halliday and Robert Resnick. *Fundamentals of physics*. John Wiley & Sons, 1981.

Kanako Hamada, Hiroshi Matsuura, Mitsuru Sanada, Futoshi Toyoda, Mariko Omatsu-Kanbe, Atsunori Kashiwagi, and Hitoshi Yasuda. Properties of the na+/k+ pump current in small neurons from adult rat dorsal root ganglia. *British journal of pharmacology*, 138(8):1517–1527, 2003.

M.A. Herrera-Valdez. Membranes with the same ion channel populations but different excitabilities. *PloS one*, 7(4):e34636, 2012.

M.A. Herrera-Valdez, E.C. McKiernan, S.D. Berger, S. Ryglewski, C. Duch, and S. Crook. Relating ion channel expression, bifurcation structure, and diverse firing patterns in a model of an identified motor neuron. *Journal of Computational Neuroscience*, pages 1–19, 2013.

Marco Arieli Herrera-Valdez. Geometry and nonlinear dynamics underlying electrophysiological phenotypes in biophysical models of membrane potential. *Dissertation. Ph.D. in Mathematics. University of Arizona*, 2014.

Marco Arieli Herrera-Valdez and Joceline Lega. Reduced models for the pacemaker dynamics of cardiac cells. *Journal of Theoretical Biology*, 270(1):164–176, 2011. doi: 10.1016/j.jtbi.2010.09.042.

B Hille. *Ionic Channels of Excitable Membranes*. Sinauer Associates, Sinauer Associates, Inc. Sunderland, Mass. 01375, 1992.

A. L. Hodgkin and A. F. Huxley. A quantitative description of membrane current and its application to conduction and excitation in nerve. *Journal of Physiology*, 117:500–544, 1952.

T. Hoshi, W. N. Zagotta, and R. W. Aldrich. Shaker potassium channel gating. I: Transitions near the open state. *Journal of General Physiology*, 103(2):249–278, 1994.

D. Johnston, S. M. S. Wu, and R. Gray. *Foundations of cellular neurophysiology*. MIT press Cambridge, MA, 1995. ISBN 0262100533.

Daniel Kaplan and Leon Glass. *Understanding nonlinear dynamics*. Springer Science & Business Media, 2012.

B Katz. Les constantes electriques de la membrane du muscle. *Arch Sci Physiol*, 3:285–299, 1949.

Douglas B Kell. On the functional proton current pathway of electron transport phosphorylation: an electrodic view. *Biochimica et Biophysica Acta (BBA)-Reviews on Bioenergetics*, 549(1):55–99, 1979.

James NC Kew and Ceri H Davies. *Ion channels: from structure to function*. Oxford University Press, USA, 2010.

Janos K Lanyi. Proton translocation mechanism and energetics in the light-driven pump bacteriorhodopsin. *Biochimica et Biophysica Acta (BBA)-Bioenergetics*, 1183(2):241–261, 1993.

P Läuger. Ion transport through pores: a rate-theory analysis. *Biochimica et Biophysica Acta (BBA)-Biomembranes*, 311(3):423–441, 1973.

PeerJ Preprints | https://doi.org/10.7287/peerj.preprints.1312v8 | CC BY 4.0 Open Access | rec: 16 Apr 2018, publ: 16 Apr 2018

Matteo E Mangoni, Brigitte Couette, Emmanuel Bourinet, Josef Platzer, Daniel Reimer, Jörg Striessnig, and Joël Nargeot. Functional role of l-type cav1. 3 ca2+ channels in cardiac pacemaker activity. *Proceedings of the National Academy of Sciences*, 100(9):5543–5548, 2003.

Matteo E Mangoni, Brigitte Couette, Laurine Marger, Emmanuel Bourinet, Jörg Striessnig, and Joël Nargeot. Voltage-dependent calcium channels and cardiac pacemaker activity: from ionic currents to genes. *Progress in biophysics and molecular biology*, 90(1):38–63, 2006.

M Mazzanti and L. J. DeFelice. Ca channel gating during cardiac action potentials. *Biophysical Journal*, 58:1059–1065, 1990.

E.C. McKiernan and M.A. Herrera-Valdez. From spinal cord to hippocampus: links between bifurcation structure, ion channel expressio n, and firing patterns in a variety of neuron types. *BMC Neuroscience*, 13(Suppl 1):P121, 2012.

Erin Christy McKiernan, Marco Arieli Herrera-Valdez, and Diano Fabio Marrone. A biophysical, minimal model to explore age-related changes in ion channel gene expression and excitability in ca1 pyramidal cells. *Society for Neurosciences Annual Meeting*, Session 628: Learning and Memory: Aging III, Poster 628.10/AA45., 2015.

C.C. Mitchell and D.G. Schaeffer. A two-current model for the dynamics of cardiac membrane. *Bulletin of mathematical biology*, 65(5):767–793, 2003. ISSN 0092-8240.

Masakazu Nakao and David C Gadsby. [na] and [k] dependence of the na/k pump current-voltage relationship in guinea pig ventricular myocytes. *The Journal of General Physiology*, 94(3):539–565, 1989.

Björn Naundorf, Fred Wolf, and Maxim Volgushev. Unique features of action potential initiation in cortical neurons. *Nature*, 440(7087):1060, 2006.

Walther Nernst. Zur kinetik der in lösung befindlichen körper. *Zeitschrift für physikalische Chemie*, 2(1): 613–637, 1888.

Wolfgang Nonner and Robert Eisenberg. Ion permeation and glutamate residues linked by poisson-nernst-planck theory in l-type calcium channels. *Biophysical Journal*, 75:1287–1305, 1998.

Lars Onsager. Reciprocal relations in irreversible processes. i. *Phys. Rev.*, 37(4):405–426, Feb 1931. doi: 10.1103/PhysRev.37.405.

David Orduz, Don Patrick Bischop, Beat Schwaller, Serge N Schiffmann, and David Gall. Parvalbumin tunes spike-timing and efferent short-term plasticity in striatal fast spiking interneurons. *The Journal of physiology*, 591(13):3215–3232, 2013.

BJ Pitts. Stoichiometry of sodium-calcium exchange in cardiac sarcolemmal vesicles. coupling to the sodium pump. *Journal of Biological Chemistry*, 254(14):6232–6235, 1979.

Max Planck. Ueber die potentialdifferenz zwischen zwei verdünnten lösungen binärer electrolyte. *Annalen der Physik*, 276(8):561–576, 1890.

Robert L Post and Philip C Jolly. The linkage of sodium, potassium, and ammonium active transport across the human erythrocyte membrane. *Biochimica et biophysica acta*, 25:118–128, 1957.

R. L. Rasmusson, J. W. Clark, W. R. Giles, K Robinson, R. B. Clark, E. F. Shibata, and D. L. Campbell. A mathematical model of electrophysiological activity in the bullfrog atrial cell. *Am. J. Physiol.*, 259: H370–H389, 1990a.

PeerJ Preprints | https://doi.org/10.7287/peerj.preprints.1312v8 | CC BY 4.0 Open Access | rec: 16 Apr 2018, publ: 16 Apr 2018

R. L. Rasmusson, J. W. Clark, W. R. Giles, E. F. Shibata, and D. L. Campbell. A mathematical model of bullfrog cardiac pacemaker cell. *Am. J. Physiol.*, 259:H352–H369, 1990b.

John P Reeves and Calvin C Hale. The stoichiometry of the cardiac sodium-calcium exchange system. *Journal of Biological Chemistry*, 259(12):7733–7739, 1984.

Robert E Ricklefs. A graphical method of fitting equations to growth curves. *Ecology*, 48(6):978–983, 1967.

Janin Riedelsberger, Ingo Dreyer, and Wendy Gonzalez. Outward rectification of voltage-gated k+ channels evolved at least twice in life history. *PloS one*, 10(9):e0137600, 2015.

J. Rinzel. Excitation dynamics: insights from simplified membrane models. In *Fed. Proc. 44*, volume 2944, 1985.

Th Rosenberg and W Wilbrandt. The kinetics of membrane transports involving chemical reactions. *Experimental cell research*, 9(1):49–67, 1955.

T. Shibasaki. Conductance and kinetics of delayed rectifier potassium channels in nodal cells of the rabbit heart. *The Journal of Physiology*, 387(1):227, 1987.

Wenying Shou, Carl T Bergstrom, Arup K Chakraborty, and Frances K Skinner. Theory, models and biology. *Elife*, 4:e07158, 2015.

J Chr SKou. Enzymatic basis for active transport of na+ and k+ across cell membrane. *Physiological Reviews*, 45(3):596–618, 1965.

Wilfred D Stein and Thomas Litman. *Channels, carriers, and pumps: an introduction to membrane transport*. Elsevier, 2014.

C. F. Stevens and R. W. Tsien. *Ion permeation through membrane channels*, volume 3. Raven Press, 1979.

S. H. Strogatz. *Nonlinear dynamics and chaos: With applications to physics, biology, chemistry, and engineering*. Westview Pr, 1994. ISBN 0738204536.

Paola Suárez, Marco Arieli Herrera-Valdez, José Bargas, and Elvira Galarraga. Un modelo biofísico de neuronas estriatales de proyección que toma en cuenta la contribución de canales de calcio cav3. *Escuela de Otoño de Biomatemáticas, Jalapa, Veracruz, México.*, 2015.

C Tanford. Equilibrium state of atp-driven ion pumps in relation to physiological ion concentration gradients. *The Journal of general physiology*, 77(2):223–229, 1981.

James M Tepper, Fatuel Tecuapetla, Tibor Koós, and Osvaldo Ibáñez-Sandoval. Heterogeneity and diversity of striatal gabaergic interneurons. *Frontiers in neuroanatomy*, 4:150, 2010.

Hans H Ussing. The active ion transport through the isolated frog skin in the light of tracer studies. *Acta Physiologica*, 17(1):1–37, 1949a.

Hans H Ussing. The distinction by means of tracers between active transport and diffusion. *Acta Physiologica*, 19(1):43–56, 1949b.

Hans H Ussing. Transport of ions across cellular membranes. *Physiological reviews*, 29(2):127–155, 1949c.

PeerJ Preprints | https://doi.org/10.7287/peerj.preprints.1312v8 | CC BY 4.0 Open Access | rec: 16 Apr 2018, publ: 16 Apr 2018

C. A. Vandenberg and F. Bezanilla. Single-channel, macroscopic, and gating currents from sodium channels in the squid giant axon. *Biophysical journal*, 60(6):1499–1510, 1991.

Jacobus Henricus van't Hoff. *Etudes de dynamique chimique*, volume 1. Muller, 1884.

P De Weer, David C Gadsby, and RF Rakowski. Voltage dependence of the na-k pump. *Annual Review of Physiology*, 50(1):225–241, 1988.

Philippa M Wiggins. The relationship between pump and leak: Part 1. application of the butler-volmer equation. *Bioelectrochemistry and Bioenergetics*, 14(4):313–326, 1985a.

Philippa M Wiggins. Relationship between pump and leak: Part 2. a model of the na, k-atpase functioning both as pump and leak. *Bioelectrochemistry and Bioenergetics*, 14(4):327–337, 1985b.

Philippa M Wiggins. Relationship between pump and leak: Part 3. electrical coupling of na+-solute uptake to the na, k-atpase. *Bioelectrochemistry and Bioenergetics*, 14(4-6):339–345, 1985c.

A. R. Willms, D. J. Baro, R. M. Harris-Warrick, and J. Guckenheimer. An improved parameter estimation method for hodgkin-huxley models. *Journal of Computational Neuroscience*, 6(2):145–168, 1999.

H Zhang, AV Holden, I Kodama, H Honjo, M Lei, T Varghese, and MR Boyett. Mathematical models of action potentials in the periphery and center of the rabbit sinoatrial node. *American Journal of Physiology-Heart and Circulatory Physiology*, 279(1):H397–H421, 2000.

PeerJ Preprints | https://doi.org/10.7287/peerj.preprints.1312v8 | CC BY 4.0 Open Access | rec: 16 Apr 2018, publ: 16 Apr 2018